to express wild-type *EML4–ALK* or one of the nine different resistance mutations. In this system, ceritinib was approximately 10-fold more potent against wild-type *EML4–ALK* than crizotinib. Whereas all these secondary mutations induced crizotinib resistance, ceritinib was potent in inhibiting the growth of Ba/F3 cells expressing four of the resistance mutations, including L1196M, G1269A, S1206Y, and I1171T (Fig. 4A; Supplementary Fig. S3; Supplementary Table S1). However, C1156Y, G1202R, 1151T-ins, L1152R, and F1174C mutations also conferred resistance to ceritinib, although ceritinib was still more potent than crizotinib against these mutations. Thus, the most common crizotinib-resistant mutations were substantially more sensitive to ceritinib than crizotinib, whereas less common resistance mutations conferred resistance to both crizotinib and ceritinib.

Structural Basis for Increased Potency of Ceritinib against *ALK* Crizotinib-Resistant Mutations

To glean insights into the structural basis for the ability of ceritinib to maintain activity toward select crizotinib-resistant mutants, the structure of the ALK catalytic domain complexed with ceritinib was determined (Fig. 4B; PDB 4MKC) and compared with the structure of the ALK catalytic domain bound to crizotinib (Fig. 4C; PDB 2XP2; ref. 16). As shown in Fig. 4A, ceritinib retains potency toward the most common G1269A and L1196M crizotinib-resistant mutants. The cocrystal structure reveals that G1269 is situated just proximal to D1270 of the activation loop DFG-motif. Although mutation to Ala in the G1269A mutant would not be predicted to present any steric obstruction to ceritinib binding, it would be predicted to introduce a steric clash to crizotinib binding due to the proximity of the phenyl ring of crizotinib. The Cl moiety of the pyrimidine hinge-binding core of ceritinib is juxtaposed with the L1196 side chain and participates in a hydrophobic interaction with the Leu side chain. In the L1196M mutant, the Cl moiety of ceritinib can interact with Met, which may compensate for the loss of interaction between Cl and the Leu side chain in wild-type ALK. In contrast, introduction of a Met at the gatekeeper position 1196 likely adversely affects crizotinib binding through both steric interference and unfavorable interactions with the 2-amino substituent of the pyridinyl hinge-binding core and the methyl substituent of the alkoxy moiety of crizotinib. These structural findings are in agreement with the increased potency of ceritinib versus crizotinib against these resistance mutations.

In contrast with G1269A and L1196M mutations, ceritinib is not potent against the G1202R crizotinib-resistant mutation (Fig. 4A). The crystal structure reveals that mutation of G1202 to a larger, bulky, and charged side chain would be incompatible with ceritinib or crizotinib ALK binding due to steric hindrance (6). This steric obstruction leads to a loss in potency as reflected by the shift in IC_{50} values observed for ceritinib and crizotinib. In contrast with the G1202R mutation, the T1151 insertion, L1152P, C1156Y, and F1174C inhibitor-resistant mutants all map to the N-terminal lobe of the ALK catalytic domain and flank opposing ends of the αC-helix. The locations of these mutants do not directly contribute to inhibitor binding in cocrystal structures. Interestingly, positions T1151 and F1174 in ALK have been previously identified as sites of activating gain-of-function mutations in neuroblastoma (17). Although difficult to predict without structural and biochemical analyses of these mutants, T1151 is adjacent to the catalytically important K1150, and insertion at this position, along with the F1174C, L1152P, and C1156Y inhibitor-resistant mutants, likely influences αC-helix mobility and conformational dynamics of the catalytic domain. Previously reported structures of nonphosphorylated ALK in the apo, ADP, and inhibitor-bound forms suggest the ALK catalytic domain structure possesses a "DFG-in" conformation (18) with a unique activation loop conformation. It is conceivable that these mutations destabilize the ALK conformation and shift the conformational equilibrium toward those that are no longer able to bind the inhibitor. It is also possible that these mutations could decrease the K_m for ATP, rendering ceritinib/crizotinib a less effective ATP competitive inhibitor.

Crizotinib-Resistant Tumors Harboring EML4–ALK Wild-Type, I1171T, or C1156Y Mutations Are Sensitive to Ceritinib *In Vivo*

To evaluate the activity of ceritinib against crizotinib-resistant tumors *in vivo*, crizotinib-resistant H2228 xenograft tumors were generated by treatment with escalating doses of crizotinib (from 50 to 100 mg/kg). Tumors that progressed during treatment with 100 mg/kg crizotinib were analyzed for resistance mechanisms. Typical tumor responses and resistance are shown for 3 animals in Supplementary Fig. S4, and are representative of the 80 animals used in this study. To determine mechanisms of resistance to crizotinib, we sequenced the ALK kinase domain of all 80 tumors and identified three distinct resistance mutations in six tumors. The G1202R, C1156Y, and I1171T mutations were detected in three, two, and one resistant tumors, respectively. Of these three mutations, G1202R and C1156Y have been previously reported in patients with NSCLC who relapsed on crizotinib (6, 7). Interestingly, I1171T has not yet been reported from crizotinib-resistant patients but was identified in an *in vitro* mutagenesis screen for resistance mutations (19).

The efficacy of ceritinib was tested against these crizotinib-resistant H2228 xenograft tumor models as well as one of the resistance models that did not harbor a resistance mutation nor *ALK* amplification (data not shown). Although each was resistant to crizotinib at 100 mg/kg, ceritinib suppressed tumor growth in multiple resistance models (Fig. 5A–D). In the wild-type and I1171T resistant models, ceritinib demonstrated impressive antitumor activity, whereas it was less active in the C1156Y-resistant model and was inactive against the G1202R-resistant model. These data are consistent with the Ba/F3 models in which ceritinib was more potent against I1171T than the C1156Y and G1202R mutants (Fig. 4A). The studies shown herein provide evidence that ceritinib can overcome resistance *in vivo*, especially in tumors harboring wild-type, L1196M, or I1171T ALK fusions at a dose that is predicted to be achievable in humans. Of note, it is rather interesting that ceritinib overcame crizotinib resistance in the

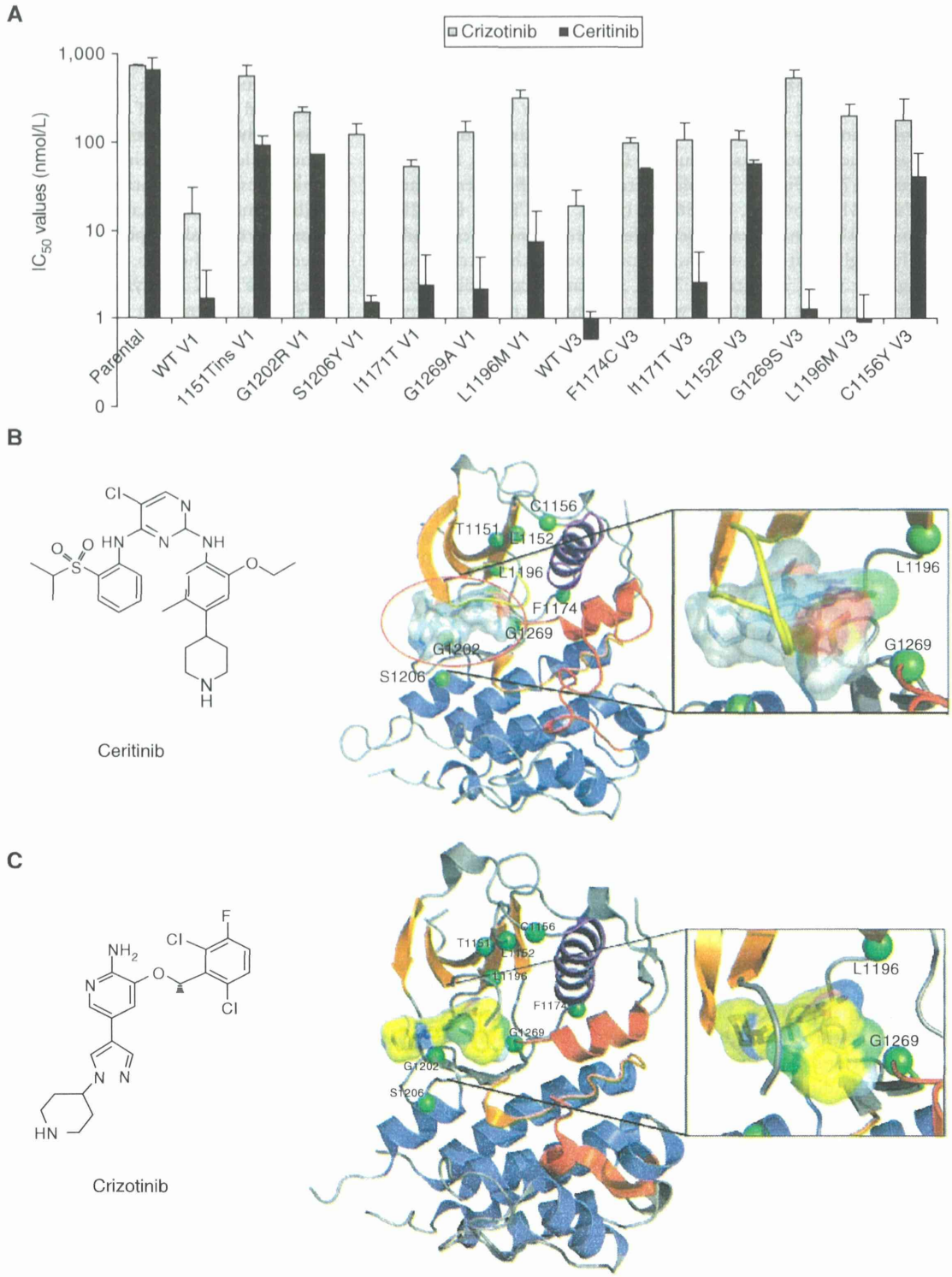

Figure 4. Ba/F3 models of ALK-crizotinib–resistant mutations. **A,** IC_{50} of ceritinib across different Ba/F3 cell lines expressing wild-type or mutated *ALK* TK and including parental, IL3-dependent Ba/F3 cells are shown. **B** and **C,** ALK-resistant mutations mapped onto ALK/ceritinib (PDB 4MKC; **B**) and ALK/crizotinib (PDB 2XP2; **C**) cocrystal structures. β-Strand secondary structural elements of the N-terminal lobe and the αC-helix of the N-terminal lobe are shown in orange and purple, respectively. Helical structural elements of the C-terminal lobe are shown in blue. Residues of the activation loop (A-loop) and catalytic loop are shown in red and orange, respectively. Residues involved in resistant mutations are depicted as green spheres. Inhibitor molecules are depicted as stick representations with carbons colored yellow and cyan for crizotinib and ceritinib, respectively. Nitrogen is colored dark blue, oxygen is colored red, and chlorine green for both inhibitors. Fluoride is colored white (crizotinib) and sulfur atoms are colored yellow (ceritinib). Transparent surfaces for the inhibitors are displayed. Zoomed-in view boxes for G1269 and L1196 residues are shown. Figures were rendered with MacPymol (The PyMOL Molecular Graphics System, Version 1.4 Schrödinger, LLC).

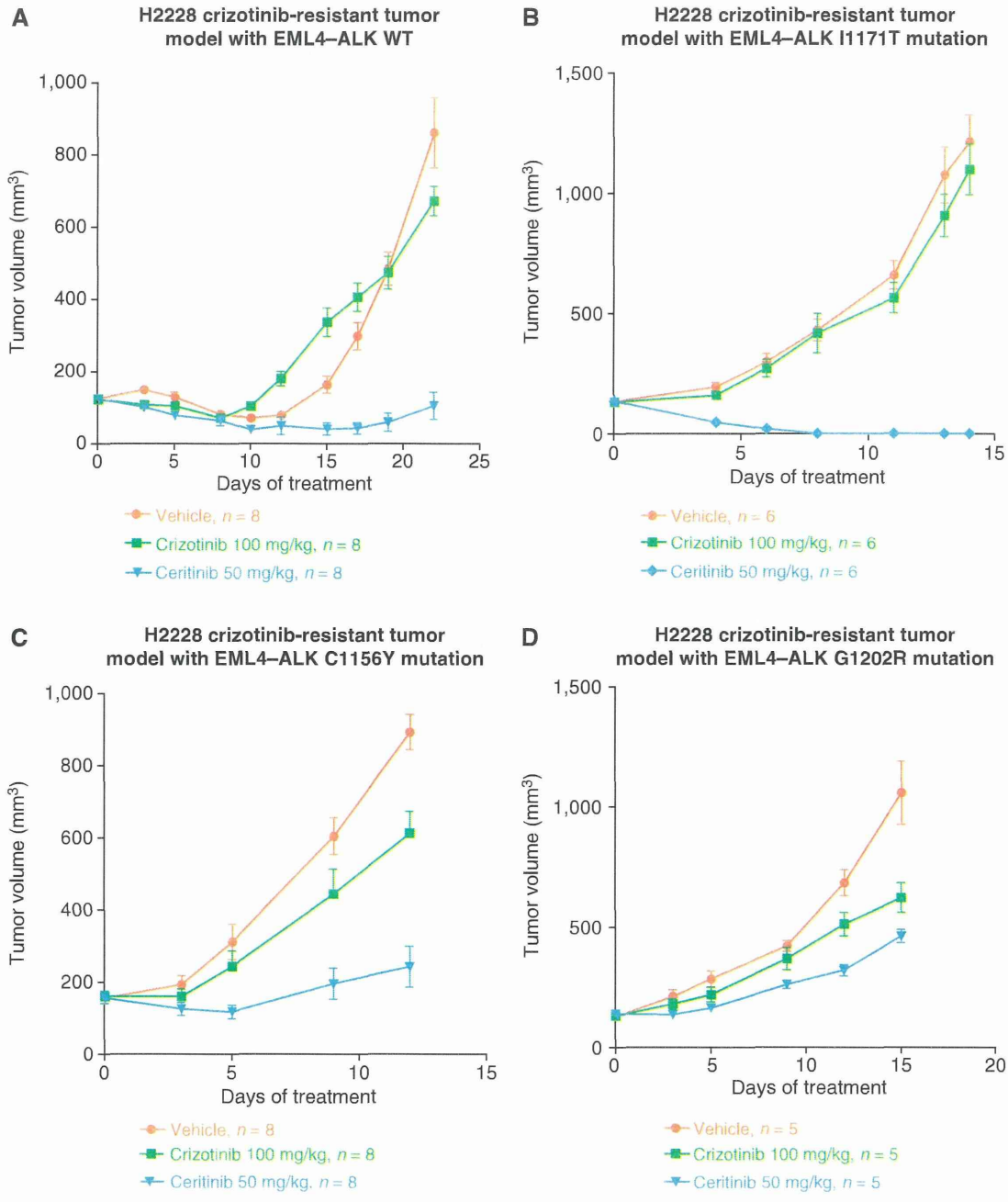

Figure 5. EML4-ALK C1156Y, I1171T, G1202R mutations' sensitivity to ceritinib. **A** to **D,** SCID beige mice bearing H2228 crizotinib-resistant tumors EML4-ALK wild-type (WT; **A**), I1171T (**B**), C1156Y (**C**), or G1202R (**D**) were treated with 100 mg/kg crizotinib or 50 mg/kg ceritinib once daily for 12 to 22 days. Tumor volumes, mean ± SD ($n = 5$–8).

tumor that did not harbor an *ALK* resistance mutation, as this recapitulates observations in the clinic and with the patient-derived cell line shown in Fig. 3 (please see "Discussion").

Acquired Resistance to Ceritinib in Patients

Ceritinib has demonstrated impressive activity in the clinic in crizotinib-resistant patients (13). However, similar to other targeted therapy successes, despite initial and durable responses, tumors do develop resistance. We have now biopsied 11 cancers with acquired resistance to ceritinib (two of which were from different sites from the same patient). As shown in Fig. 6A, five of these biopsies revealed the development of mutations at either G1202 or F1174 in the ceritinib-resistant cancers. In the patient JFCR021, who had two sites of disease biopsied, two different ceritinib-resistant mutations were identified, underscoring the heterogeneity of resistance mechanisms that can be identified in a single patient (6). Of

A

Patient ID	*EML4–ALK* sequence at crizotinib resistance	*EML4–ALK* sequence at ceritinib resistance
MGH011	S1206Y	G1202R
MGH015	WT	WT
MGH023	WT	F1174C
MGH034	WT	WT
MGH049	WT	WT
MGH051	WT	G1202R
MGH057	N/A	WT
MGH061	WT	WT
JFCR013	N/A	WT
JFCR021	G1269A (right lung)	F1174V (left lung) and G1202R (right lung)

B

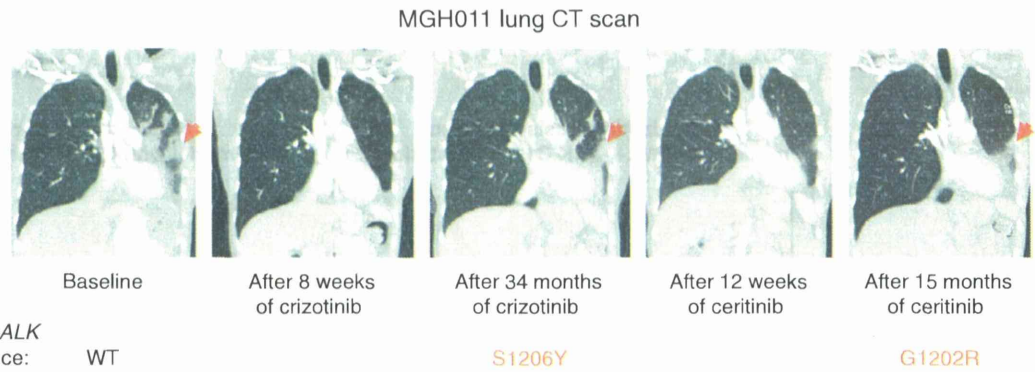

Figure 6. Ceritinib-resistant tumors acquired mutations at positions G1202 or F1174. **A,** ALK mutational status in ceritinib-resistant patient tumors before and after ceritinib treatment. **B,** thoracic computed tomography (CT) images of patient MGH011 during crizotinib or ceritinib treatments. Sites of biopsies (red arrows) revealed the presence of different *ALK* secondary mutations throughout the treatments. Tumor growth observed during ceritinib treatment is consistent with disease progression. WT, wild-type.

note, 2 of the patients had crizotinib-resistant mutations before enrolling on ceritinib (MGH011; Fig. 6B; and JFCR021) that our laboratory studies suggested would be sensitive to ceritinib. In the ceritinib-resistant cancers, those mutations were no longer detected, but the G1202R mutation emerged (Fig. 6B). These findings are consistent with preclinical studies presented in this article demonstrating the activity of ceritinib against G1269A and S1206Y crizotinib-resistant mutations, and its lack of potency against the G1202R mutation.

DISCUSSION

Since its approval in the United States in 2011, the ALK inhibitor crizotinib has emerged as a standard of care for patients with advanced NSCLC harboring the *ALK* fusion oncogene. Unfortunately, as has been observed with other targeted therapies, the emergence of resistance has ultimately limited the benefit of this therapy. Next-generation ALK inhibitors (ceritinib, CH5424802, ASP3026, AP26113, and X-396) have been developed with the hope that they may overcome acquired resistance to crizotinib. We previously reported differential activity of some of these ALK inhibitors depending on the resistance mutations present within the ALK TK domain (6, 11). In an ongoing early-phase clinical study, ceritinib has exhibited dramatic activity in patients with ALK-rearranged NSCLC (13).

In these studies, we find that ceritinib is a more potent ALK inhibitor than crizotinib, and has marked activity in crizotinib-naïve models of *ALK*-positive NSCLC, including H2228, H3122, and Ba/F3 cell lines *in vitro* and MGH006 primary explants *in vivo*. To better characterize the activity of ceritinib in crizotinib resistance, we developed a variety of crizotinib-resistant models, including cell lines derived from biopsies from patients whose cancers had developed resistance to crizotinib in the clinic. These models harbored different resistance mechanisms, including various *ALK* resistance mutations. The activity of ceritinib varied depending on the specific *ALK* resistance mutation. For example, in Ba/F3 models, ceritinib was highly active against L1196M, G1269A, S1206Y, and I1171T EML4–ALK mutants, and less active against the less common mutations C1156Y, G1202R, 1151T-ins, L1152P, and F1174C. It is notable that in the phase I

study of ceritinib, five of 19 crizotinib-resistant tumors harbored resistance mutations at residues 1196, 1269, and 1206, with one tumor harboring both G1269A and 1151T-ins. The patients harboring these resistance mutations all exhibited significant tumor shrinkage (13).

Importantly, as has been observed in the clinic, ceritinib showed potent efficacy *in vitro* and *in vivo* against a crizotinib-resistant tumor that did not harbor an *ALK* resistance mutation or gene amplification (Fig. 3B). Interestingly, the patient-derived cell line also retained sensitivity to crizotinib *in vitro*, demonstrating that these cells are still sensitive to ALK inhibition. One potential explanation for this finding is that, in the clinic, crizotinib fails to achieve tumor levels that completely inhibit ALK, and that tumor cells can survive through modest input from activation of bypass tracks such as EGFR. However, these cells remain sensitive to complete ALK inhibition. In the setting of a more potent ALK inhibitor, ALK is inhibited fully, abrogating the functional role of bypass tracks and leading to the elimination of tumor cells. It is also possible that this patient relapsed on crizotinib because of poor adherence to therapy or due to a stromal contribution. Similar findings were also observed in the H2228 xenograft model that developed resistance to crizotinib *in vivo*, did not develop an *ALK* mutation, and was sensitive to ceritinib (Fig. 5A). These findings may explain, at least in part, the finding that ceritinib is highly active in crizotinib-resistant cancers with or without *ALK* resistance mutations.

The initial interrogation of ceritinib-resistant patient biopsies supports the notion that ceritinib is able to effectively suppress many crizotinib-resistant mutations, but the G1202R and F1174V/C mutants are resistant to ceritinib. It is noteworthy that in two cases, the crizotinib-resistant mutations, S1206Y and G1269A, were no longer observed in the ceritinib-resistant biopsies in which the G1202R mutations were observed (Fig. 6A). This suggests that predominant clones with the S1206Y and G1269A mutations were suppressed by ceritinib, whereas much more rare clones with G1202R mutations were selected by ceritinib. These findings give further support to the notion that there are multiple populations of resistant clones whose emergence is dependent on the selective pressure applied.

Altogether, our *in vitro* and *in vivo* data, including cell line models established from crizotinib-resistant patient samples, demonstrate that the next-generation ALK inhibitor ceritinib is active against most crizotinib-resistant tumors. This is consistent with the marked clinical activity of ceritinib in patients with *ALK*-positive NSCLC who progressed on crizotinib. As resistance to ceritinib has already been observed in the clinic, future studies will need to identify mechanisms of resistance to ceritinib other than mutations in the G1202 and F1174 residues to maximize the clinical benefit afforded by next-generation ALK-targeted therapies.

METHODS

Cell Lines and Reagents

All human lung cancer samples were obtained from patients with informed consent at the Massachusetts General Hospital (MGH) and the Japanese foundation for Cancer Research (JFCR), and all procedures were conducted under an Institutional Review Board (IRB)–approved protocol. Cells in pleural effusion were collected by centrifugation at 440 × *g* for 10 minutes. After red blood cells were lysed with the Red Blood Cell Lysis Solution (BioLegend), cells were grown in ACL-4 (Invitrogen) supplemented with 1% FBS or RPMI-1640 supplemented with 10% FBS and 1× Antibiotic-Antimycotic. After the cells started growing stably, clonal cell lines were also established.

H3122, H2228, A549, H460, H1299, HCC827, and H522 cell lines were provided by the Center for Molecular Therapeutics (CMT) at Massachusetts General Hospital (Boston, MA), which performs routine cell line authentication testing by single-nucleotide polymorphism and short-tandem repeat analysis. BT-474, SKBR3, and the *ALK*-positive patient-derived cell lines used in this study are from the Engelman laboratory (Boston, MA) and have been previously tested for mutation status to confirm their authenticity. A549, H460, H1299, HCC827, H522, SKBR3, H2228, H3122, H3122 CR1, and MGH021-4 cell lines were cultured in RPMI-1640 supplemented with 10% FBS. For survival assays, H2228 were cultured in 1% FBS. The MGH045 cell line was cultured in ACL-4 supplemented with 1% FBS, and MGH051 and BT-474 were cultured in DMEM supplemented with 10% FBS.

Mouse myeloma Ba/F3 cells were cultured in DMEM supplemented with 10% FBS with (parental) or without (EML4–ALK) IL3 (0.5 ng/mL). cDNAs encoding *EML4–ALK* variant1 or *EML4–ALK* variant3 containing different point mutations were cloned into retroviral expression vectors, and virus was produced as previously described (11). After retroviral infection, Ba/F3 cells were selected in puromycin (0.5 μg/mL) for 2 weeks. IL3 was withdrawn from the culture medium for more than 2 weeks before experiments.

Crizotinib was purchased from ChemieTek, and ceritinib was provided by Novartis. Both were dissolved in DMSO for *in vitro* experiments. Ceritinib was formulated in 0.5% methyl cellulose/0.5% Tween 80 and crizotinib in 0.1 N HCl or 0.5% methyl cellulose/0.5% Tween 80 for *in vivo* studies.

Western Blot Analysis

A total of 5×10^5 cells were treated in 6-well plates for 6 hours with the indicated drugs. Cell protein lysates were prepared as previously described (6, 11). Phospho-ERK (T202/Y204), ERK, S6, phospho-S6, phospho-AKT (S473 and T308), AKT, phospho-ALK (Y1282/1283), and ALK antibodies were obtained from Cell Signaling Technology. GAPDH was purchased from Millipore.

Survival Assays

Cells (2,000 or 5,000) were plated in triplicate into 96-well plates. Seventy-two hours (48 hours for Ba/F3 cells and 7 days for MGH051) after drug treatments, cells were incubated with a CellTiter-Glo assay reagent (Promega) for 15 minutes, and luminescence was measured with a Centro LB 960 Microplate Luminometer (Berthold Technologies).

In Vivo Efficacy Study of Ceritinib

SCID beige mice for crizotinib-resistant H2228 xenograft tumor models, nude mice for MGH006 primary explants and MGH045 cells were randomized into groups of 5, 6, or 8 mice with an average tumor volume of approximately 150 mm^3 and received crizotinib or ceritinib daily treatments by oral gavage as indicated in each study. Tumor volumes were determined by using caliper measurements and calculated with the formula (length × width × height)/2.

In Vitro Enzymatic Assay

An enzymatic assay for the recombinant ALK kinase domain (1066–1459) was conducted using the Caliper mobility shift methodology, using fluorescently labeled peptides as kinase substrates. The

Caliper assay was performed at 30°C for 60 minutes in a total volume of 9 μL. The reaction was terminated by the addition of 16 μL of stop solution [100 mmol/L HEPES, 5% (v/v) DMSO, 0.1% (v/v) coating reagent, 10 mmol/L EDTA, 0.015% (v/v) Brij 35]. After termination of the reactions, the plates were transferred into the Caliper LabChip 3000 workstation for analysis.

Analysis of ALK/Ceritinib and ALK/Crizotinib Costructures

The ALK/ceritinib costructure was determined by the soaking of 2 mmol/L ceritinib into apo crystals grown in 0.2 mol/L sodium acetate trihydrate/20% PEG3350 using protein expressed and purified as previously described (18). The ALK/ceritinib final model determined to 2.0 Å (PDB 4MKC on hold) was superimposed with the coordinates of the ALK/crizotinib costructure (PDB 2XP2) for analyses.

Patient Sample Analyses

The patients with ALK-positive NSCLC with acquired ceritinib resistance underwent biopsy of their resistant tumors between January 2011 and September 2013. Standard histopathology was performed to confirm the diagnosis of malignancy as previously described (6). The electronic medical record was reviewed retrospectively to obtain clinical information under an IRB-approved protocol. This study was approved by the IRB of MGH or the Cancer Institute Hospital of JFCR.

Disclosure of Potential Conflicts of Interest

M. Nishio has received honoraria from the speakers' bureaus of Pfizer and Chugia Pharmaceutical Co., Ltd. A.T. Shaw is a consultant/advisory board member of Novartis, Pfizer, and ARIAD. J.A. Engelman has received commercial research grants from Novartis and Sanofi-Aventis, and is a consultant/advisory board member of Novartis, Sanofi-Aventis, Chugia Pharmaceutical Co., Ltd., and Ventana Medical Systems, Inc. No potential conflicts of interest were disclosed by the other authors.

Authors' Contributions

Conception and design: L. Friboulet, N. Li, P.-Y. Michellys, M.M. Awad, A.C. Pferdekamper, S. Kasibhatla, F. Sun, J.L. Harris, A.T. Shaw, J.A. Engelman

Development of methodology: L. Friboulet, R. Katayama, M.M. Awad, S. Kim, A.C. Pferdekamper, J. Li, S. Kasibhatla, F. Sun, S. Mahmood, E.L. Lockerman, N. Fujita

Acquisition of data (provided animals, acquired and managed patients, provided facilities, etc.): L. Friboulet, R. Katayama, C.C. Lee, J.F. Gainor, A.S. Crystal, N.Yanagitani, A.C. Pferdekamper, F. Sun, X. Sun, S. Hua, P. McNamara, M. Nishio, A.T. Shaw

Analysis and interpretation of data (e.g., statistical analysis, biostatistics, computational analysis): L. Friboulet, N. Li, R. Katayama, C.C. Lee, J.F. Gainor, M.M. Awad, N.Yanagitani, A.C. Pferdekamper, S. Kasibhatla, F. Sun, P. McNamara, J.L. Harris, A.T. Shaw, J.A. Engelman

Writing, review, and/or revision of the manuscript: L. Friboulet, N. Li, R. Katayama, C.C. Lee, J.F. Gainor, A.S. Crystal, M.M. Awad, J.L. Harris, A.T. Shaw, J.A. Engelman

Administrative, technical, or material support (i.e., reporting or organizing data, constructing databases): R. Katayama, A.C. Pferdekamper, S. Mahmood, E.L. Lockerman, N. Fujita, M. Nishio, J.A. Engelman

Study supervision: N. Li, S. Kasibhatla, M. Nishio, A.T. Shaw, J.A. Engelman

Acknowledgments

The authors thank Thomas Marsilje, Celin Tompkins, and Auzon Steffy for expert technical assistance and input on the studies described in the article; Atsushi Horiike for helping to obtain repeat biopsy samples; and Be a Piece of the Solution and the Evan Spirito Memorial Foundation for support of lung cancer research at MGH.

Grant Support

This work was supported by a grant from the NIH (5R01CA164273-02 to A.T. Shaw and J.A. Engelman), by a V Foundation Translational Research Grant (to A.T. Shaw and J.A. Engelman) and by the NIH/National Cancer Institute (R01CA137008 to J.A. Engelman). The study was also supported by a grant from JSPS KAKENHI (25710015 to R. Katayama).

Received November 5, 2013; revised March 12, 2014; accepted March 19, 2014; published OnlineFirst March 27, 2014.

REFERENCES

1. Kwak EL, Bang YJ, Camidge DR, Shaw AT, Solomon B, Maki R, et al. Anaplastic lymphoma kinase inhibition in non-small-cell lung cancer. N Engl J Med 2010;363:1693–703.
2. Soda M, Choi YL, Enomoto M, Takada S, Yamashita Y, Ishikawa S, et al. Identification of the transforming EML4-ALK fusion gene in non-small-cell lung cancer. Nature 2007;448:561–6.
3. Koivunen JP, Mermel C, Zejnullahu K, Murphy C, Lifshits E, Holmes AJ, et al. EML4-ALK fusion gene and efficacy of an ALK kinase inhibitor in lung cancer. Clin Cancer Res 2008;14:4275–83.
4. Doebele RC, Pilling AB, Aisner DL, Kutateladze TG, Le AT, Weickhardt AJ, et al. Mechanisms of resistance to crizotinib in patients with ALK gene rearranged non-small cell lung cancer. Clin Cancer Res 2012;18:1472–82.
5. Gainor JF, Varghese AM, Ou SH, Kabraji S, Awad MM, Katayama R, et al. ALK rearrangements are mutually exclusive with mutations in EGFR or KRAS: an analysis of 1,683 patients with non-small cell lung cancer. Clin Cancer Res 2013;19:4273–81.
6. Katayama R, Shaw AT, Khan TM, Mino-Kenudson M, Solomon BJ, Halmos B, et al. Mechanisms of acquired crizotinib resistance in ALK-rearranged lung Cancers. Sci Transl Med 2012;4:120ra117.
7. Choi YL, Soda M, Yamashita Y, Ueno T, Takashima J, Nakajima T, et al. EML4-ALK mutations in lung cancer that confer resistance to ALK inhibitors. N Engl J Med 2010;363:1734–9.
8. Lovly CM, Pao W. Escaping ALK inhibition: mechanisms of and strategies to overcome resistance. Sci Transl Med 2012;4:120ps122.
9. Sasaki T, Koivunen J, Ogino A, Yanagita M, Nikiforow S, Zheng W, et al. A novel ALK secondary mutation and EGFR signaling cause resistance to ALK kinase inhibitors. Cancer Res 2011;71:6051–60.
10. Sasaki T, Okuda K, Zheng W, Butrynski J, Capelletti M, Wang L, et al. The neuroblastoma-associated F1174L ALK mutation causes resistance to an ALK kinase inhibitor in ALK-translocated cancers. Cancer Res 2010;70:10038–43.
11. Katayama R, Khan TM, Benes C, Lifshits E, Ebi H, Rivera VM, et al. Therapeutic strategies to overcome crizotinib resistance in non-small cell lung cancers harboring the fusion oncogene EML4-ALK. Proc Natl Acad Sci U S A 2011;108:7535–40.
12. Marsilje TH, Pei W, Chen B, Lu W, Uno T, Jin Y, et al. Synthesis, structure-activity relationships, and *in vivo* efficacy of the novel potent and selective anaplastic lymphoma kinase (ALK) inhibitor 5-Chloro-N2-(2-isopropoxy-5-methyl-4-(piperidin-4-yl)phenyl)-N4-(2-(isopropylsulfonyl)phenyl)pyrimidine-2,4-diamine (LDK378) currently in phase 1 and phase 2 clinical trials. J Med Chem 2013;56:5675–90.
13. Shaw AT, Kim DW, Mehra R, Tan DS, Felip E, Chow LQ, et al. Ceritinib in ALK-rearranged non-small-cell lung cancer. N Engl J Med 2014;370:1189–97.
14. Early Results Promising for LKD378 in ALK-positive NSCLC. Cancer Discov 2013;3:OF5.
15. FDA, Center for Drug Evaluation and Research. 2011Application Number: 202570Orig1s000; Reference ID: 3006911.
16. Cui JJ, Tran-Dube M, Shen H, Nambu M, Kung PP, Pairish M, et al. Structure based drug design of crizotinib (PF-02341066), a potent

and selective dual inhibitor of mesenchymal-epithelial transition factor (c-MET) kinase and anaplastic lymphoma kinase (ALK). J Med Chem 2010;54:6342–63.
17. Chand D, Yamazaki Y, Ruuth K, Schonherr C, Martinsson T, Kogner P, et al. Cell culture and Drosophila model systems define three classes of anaplastic lymphoma kinase mutations in neuroblastoma. Dis Models & Mech 2013;6:373–82.
18. Lee CC, Jia Y, Li N, Sun X, Ng K, Ambing E, et al. Crystal structure of the ALK (anaplastic lymphoma kinase) catalytic domain. Biochem J 2010;430:425–37.
19. Zhang S, Wang F, Keats J, Zhu X, Ning Y, Wardwell SD, et al. Crizotinib-resistant mutants of EML4-ALK identified through an accelerated mutagenesis screen. Chem Biol Drug Des 2011;78:999–1005.

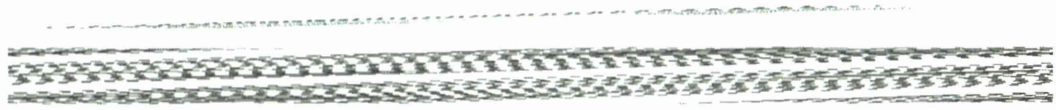

The ALK Inhibitor Ceritinib Overcomes Crizotinib Resistance in Non–Small Cell Lung Cancer

Luc Friboulet, Nanxin Li, Ryohei Katayama, et al.

Cancer Discovery 2014;4:662-673. Published OnlineFirst March 27, 2014.